

Low-Energy Electron Attachment to 5'-Thymidine Monophosphate: Modeling Single Strand Breaks Through Dissociative Electron Attachment

Anil Kumar and Michael D. Sevilla*

Department of Chemistry, Oakland University, Rochester, Michigan 48309

Received: January 30, 2007; In Final Form: March 6, 2007

Mechanisms of low-energy electron (LEE) attachment and subsequent single-strand break (SSB) formation are investigated by density functional theory treatment of a simple model for DNA, i.e., the nucleotide, 5'-thymidine monophosphate (5'-dTMPH). In the present study, the C_{5'}–O_{5'} bond dissociation due to LEE attachment has been followed along the adiabatic as well as on the vertical (electron attached to the optimized geometry of the neutral molecule) anionic surfaces using B3LYP functional and 6-31G* and 6-31++G** basis sets. Surprisingly, it is found that the PES of C_{5'}–O_{5'} bond dissociation in the anion radicals have approximately the same barrier for both adiabatic and vertical pathways. These results provide support for the hypothesis that transiently bound electrons (shape resonances) to the virtual molecular orbitals of the neutral molecule likely play a key role in the cleavage of the sugar–phosphate C_{5'}–O_{5'} bond in DNA resulting in the direct formation of single strand breaks without significant molecular relaxation. To take into account the solvation effects, we considered the neutral and anion radical of 5'-dTMP surrounded by 5 or 11 water molecules with Na⁺ as a counterion. These structures were optimized using the B3LYP/6-31G** level of theory. We find the barrier height for adiabatic C_{5'}–O_{5'} bond dissociation of 5'-dTMP anion radical in aqueous environment is so substantially higher than in the gas phase that the adiabatic route will not contribute to DNA strand cleavage in aqueous systems. This result is in agreement with experiment.

Introduction

DNA damage caused by attachment of low-energy electrons (LEEs) to DNA is increasingly recognized as a significant contributor to cellular radiation damage.^{1–3} LEEs with energies below 15 eV are produced in a large quantity (4×10^4 per MeV energy deposited)⁴ along the tracks of the ionizing radiation. The recent discovery made by Sanche's group⁴ that LEEs can induce strand breaks in DNA even below 4 eV attracted intense interest by the scientific community in elucidation of the mechanism of action. LEEs have been found to modify DNA components, e.g., bases, sugar, and phosphate by capture and creation of transient radical anions leading to dissociative electron attachment (DEA).^{4,5a,5b} Recent experiments confirm that LEEs even in the subexcitation energy range of 0.1–3 eV leads to a variety of chemical reactions in DNA and its components. These include: hydrogen atom loss,^{6a} single-strand breaks (SSBs),^{4a,4b} glycosidic bond cleavage,^{4b,4c,6} and the fragmentation of deoxyribose.⁷ We note that while LEEs clearly result in DNA strand breaks, it has been long known that in aqueous solution solvated electron attachment to DNA does not cause strand breaks even though the pyrimidine DNA base anion radical intermediates are formed.^{1b–1d}

In recent years, several groups have made efforts to understand details of the mechanism of LEE induced DNA strand breaks using both experimental^{4,6,7} and theoretical^{8–17} approaches and electron molecule interaction.^{15–21} Simons and co-workers proposed the first model for LEE cleavage of the DNA strand,¹³ which they have further delineated in subsequent work.^{9–14} In their model, they suggest the C–O bond cleavage in 5'-dTMP and 5'-dCMP captures an electron (shape resonance) and proceeds on the adiabatic surface^{11,13} with the LEE initially trapped into the π^* orbital of the base rather than phosphate

group. They proposed the “electron induced” mechanism¹⁰ of C–O sugar–phosphate bond dissociation. In their treatment, they used Hartree–Fock (HF) method and 6-31+G* basis set.¹³ The calculated gas-phase electron affinities (EAs) of their models showed negative electron affinities,^{10–14} owing to the small basis sets employed. Positive adiabatic electron affinities of nucleotides and nucleosides have been predicted by higher level calculations.^{8,15–21} For the pyrimidine DNA bases, only dipole bound anion radicals have been observed experimentally,^{22,23} having electron affinities 93 ± 7 and 62 ± 8 meV for uracil and thymine, suggesting that the valence adiabatic EAs are lower than these values.

An second model for DNA strand breaks was proposed by Li et al.^{8d} using density functional B3LYP/6-31+G(d) and the ONIOM method. To eliminate electron attachment to the DNA bases which have higher electron affinity than the DNA backbone, the model chosen was a sugar–phosphate–sugar structure without the DNA bases. They^{8d} calculated the barrier height of ~ 10 kcal/mol to dissociate the C–O bond both at 3'- and 5'- sites. Recently, using several basis sets, Li et al.^{8b} calculated the spin density distribution of the excess electron in this sugar–phosphate–sugar model,^{8d} and they found the starting state was not a valence bound state but “dipole bound” anionic state.^{8b} This model^{8d} thus gives the energy of the cleavage from a weakly associated electron not in a valence state until its capture at the transition state.

Recently, using B3LYP/DZP++ level of theory, Leszczynski and co-workers^{16,17} considered the similar model to Simons and co-workers¹³ and calculated the adiabatic transition states for the C_{3'}–O_{3'} and C_{5'}–O_{5'} σ bond dissociation in pyrimidine nucleotide anion radicals and found a barrier height of ~ 14.0 kcal/mol (C_{5'}–O_{5'} bond cleavage). Their calculations^{16,17} pre-

dicted the initial localization of the excess electron in the π^* orbital of the pyrimidine, which subsequently transfers to the σ^* orbital of the C–O bond when the bond is stretched to the transition state distance. As mentioned above, it is well-known that in an aqueous environment once an electron is stabilized on the DNA base no significant strand cleavage reactions occurs,^{1b–1d} for this reason the time frame for the transfer of electron to promote strand cleavage must be short and most likely occurs during the transient absorption event not on the adiabatic surface.

Recently, the experimental findings of Märk, Illenberger and co-workers,^{7,24} for the decomposition of D-ribose⁷ and thymidine²⁴ by low-energy electrons (LEEs), showed that migration of the excess charge from the π^* orbital of the anion of the nucleobase to DNA backbone is inhibited and may hence not contribute to SSBs as proposed by Simons et al.^{9–14} Further, they proposed that the direct mechanism of single strand breaks occurring in DNA at subexcitation energies (<4 eV) is due to dissociative electron attachment (DEA) directly to the phosphate group.²⁵ They also proposed that LEE may trap into the virtual MO of the phosphate group which is characterized as “shape resonance”.²⁵ The “shape resonance” or “single-particle resonance” occurs when an incident electron is temporarily attach to the potential connected with the ground electronic state of the molecule.²⁶ These resonances occur at low energies (0–4 eV)²⁶ and have a life time in the range 10^{-10} – 10^{-15} s. There are several pathways for the decay of the resonance state of the molecule such as vibrational and rotational levels of molecule, electronic excitation, elastic scattering, and dissociative electron attachment (DEA).²⁶ In the case of plasmid DNA, Sanche et al.^{4b} also found that LEE result in formation of well-localized transient anionic states (resonances) leading to SSBs and DSBs. The temporary anion state formation and dissociative electron attachment (DEA) mechanisms have been elucidated in diatomic molecules²⁶ and recently for larger molecular systems.²⁷

The work of Aflatooni et al.²⁸ regarding the electron attachment energies of the DNA bases, using low-energy electron transmission spectroscopy (ETS), found resonance peaks in the electron scattering cross sections due to the formation of temporary anionic states.²⁸ Their assigned vertical attachment energies (VAEs) to the DNA bases are also in good agreement with the theoretically calculated VAEs of bases by Sevilla et al.²⁹ They also observed the evidence of the nuclear motion of the temporary formed anions associated with the lowest unoccupied molecular orbitals (LUMOs) of the bases which demonstrated that electrons in the LUMOs strongly excites the vibrational modes of the neutral molecules. Recently, Burrow and co-workers analyzed³⁰ the uracil and thymine structures appearing in DEA and electron transmission spectroscopy (ETS) as vibrational Feshbach resonances (VFRs), which arises from coupling between the dipole bound state and the temporary anion state associated with occupation of lowest σ^* orbital near N1-H bond.³⁰

The recent high level calculations^{16,17} on electron addition to 5'-dTMPH discussed above have followed the adiabatic potential energy surface, which may not be the appropriate model for bond cleavage by LEEs since dissociation likely occurs before full relaxation takes place. In this work we have chosen to calculate the potential energy surface (PES) of the dissociation of C_{5'}–O_{5'} σ bond of 5'-thymidine monophosphate nucleotide (5'-dTMPH) anion radical following both the adiabatic and the vertical potential energy surfaces. Comparison of the vertical and adiabatic PES barrier heights as well as the nature of the electron distribution in two cases aids in elucidation

TABLE 1: Adiabatic (AEA) and Vertical (VEA) Electron Affinities (eV) of 5'-dTMPH Calculated Using B3LYP Method and Different Basis Sets

method	system	AEA	“VEA”	VDE ^a
B3LYP/6-31G ^{*b}	5'-dTMPH	−0.35 (−0.21) ^c	−1.06 ^c	
B3LYP/6-31++G ^{**b}	5'-dTMPH	0.25 (0.40)	0.04 ^d	0.97
B3LYP/DZP++ ^e	5'-dTMPH	0.28 (0.44)	0.01	0.99
B3LYP/6-31G ^{*b}	5'-dTMPNa	1.20	0.30	2.60
	+11 H ₂ O			
B3LYP/6-31G ^{*b}	5'-dTMPNa	2.17 ^f	1.33 ^f	3.20 ^f
PCM model	+11 H ₂ O			
B3LYP/DZP++ ^g	5'-dTMPH	2.00	1.44	2.47
IPCM model (ref 38)				

^a Vertical detachment energy (VDE) calculated as the difference between the total energy of the neutral molecule calculated at the optimized geometry of the anion and the total energy of the optimized anion. ^b Present calculation ^c The zero-point corrected values are given in parentheses. The values for 6-31G* are not good indications of the AEA or the VEA owing to the small size of the basis set. ^d This value is not a reliable calculation of the valence VEA as it is near zero and diffuse states (dipole bound and continuum) mix with the valence state. It is presented here for comparison to other work. ^e Ref 16 ^f Single-point calculation using polarized continuum model (PCM) considering water as solvent with $\epsilon = 78.39$. ^g IPCM model using water as solvent ($\epsilon = 78.39$). Ref 38

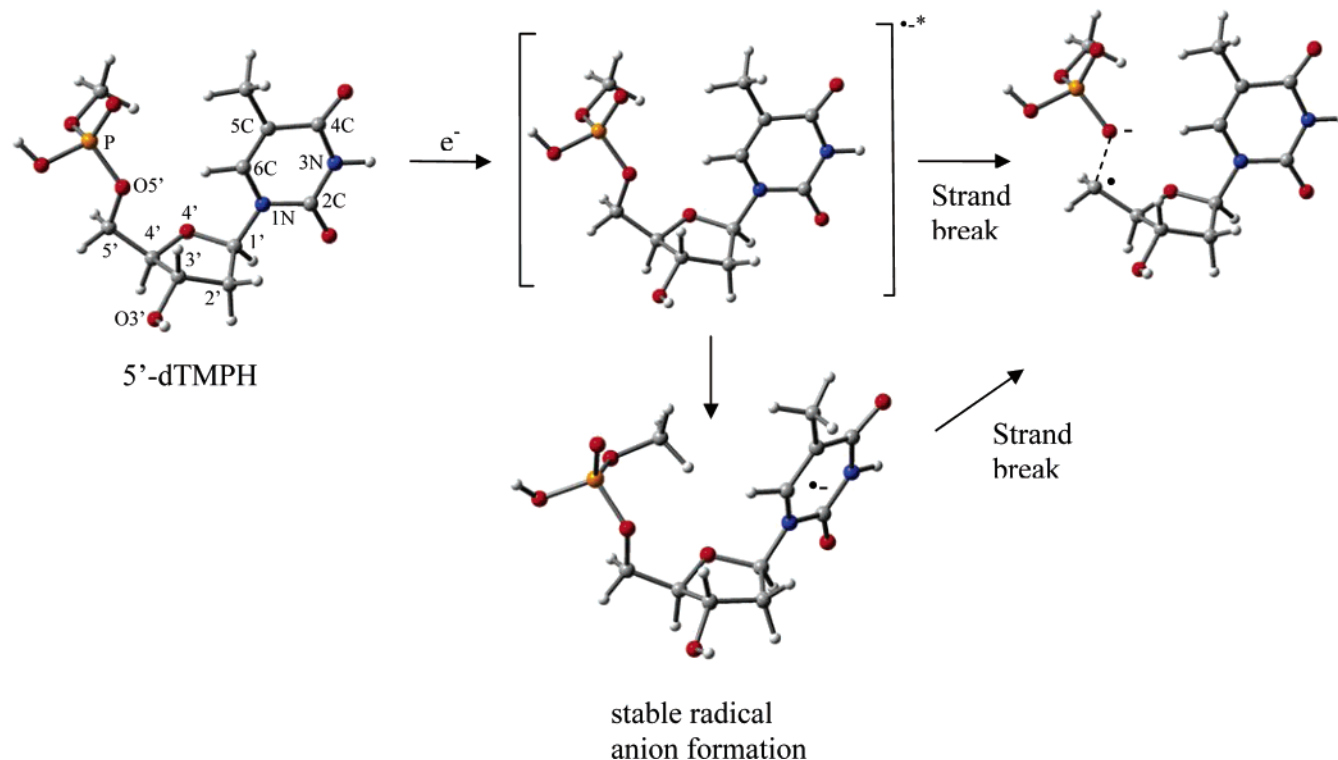
of possible C_{5'}–O_{5'} bond dissociation. Further, we better approximate an adiabatic pathway toward bond dissociation in the aqueous environment by considering the anion radical of 5'-dTMP surrounded by eleven water molecules and Na⁺ as a counterion which results in a very large barrier height for C_{5'}–O_{5'} bond dissociation.

Methods of Calculation

The geometries of 5'-dTMPH in its neutral and anionic states were optimized using density functional theory. The B3LYP functional and 6-31G* and 6-31++G** basis sets were used in this work. We also note at this level of theory AEAs are overestimated by ~0.15 eV.¹⁹ Vibrational frequencies of the neutral, anionic radical, and transition state (TS) structure of 5'-dTMPH were also calculated using this same method and basis sets. It is found that computed properties of a radical anion very much depend on the method and basis set chosen.¹⁹ Recently, Schaefer and his co-workers³¹ devised a DZP++ basis set to study the electron affinities (EAs) of a number of radical anions. They found that B3LYP functional with DZP++ basis set is a good choice.^{16–18,31} In the present study, we found that both B3LYP/DZP++ and B3LYP/6-31++G** methods gave similar results regarding the molecular geometries of neutral and anion, EA and transition state (TS) structure for the breaking of C_{5'}–O_{5'} σ bond of 5'-dTMPH radical anion. In the present calculation of the 5'-dTMPH, the phosphate group attached to the 5'- end of the thymidine was terminated by the CH₃ group, the oxygen atom at 3'- end was terminated by the hydrogen atom and the anionic phosphate group was protonated to neutralize the system (as shown in Scheme 1). All the calculations were done using Gaussian 03 suite of programs.³² Molecular orbitals were plotted using GaussView molecular modeling software,³³ while JMOL program³⁴ was used to draw the molecular structures. The adiabatic electron affinity (AEA) of a molecule is calculated as

$$\text{AEA} = T^{\text{neutral}} - T^{\text{anion}}$$

where T^{neutral} and T^{anion} are the total energies of the molecule in their neutral and a optimized states, respectively. The vertical electron affinity (VEA) is calculated as the difference between

SCHEME 1: Proposed Mechanism of Single Strand Break (SSB) Due to Attachment of LEE with 5'-dTMPH Molecule

the total energy of the optimized neutral molecule and the total energy of the corresponding anion calculated at the optimized geometry of the neutral molecule. In this work we provide theoretical calculations which provide a rationale for why LEEs can induce strand breaks but aqueous electrons cannot.

Results and Discussion

The atom numbering scheme and the proposed mechanism of single strand breaks (SSBs) due to attachment of LEE to the 5'-dTMPH molecule is shown in Scheme 1. In the proposed Scheme 1, two possible pathways of strand breaks are shown: (i) the LEE attaches to the neutral molecule transiently (resulting in a temporary anion formation or a "shape resonance") and strand breaks occur perhaps through vibrational excitation in this resonance (time scale $< 10^{-13}$ s) and (ii) the transiently bound LEE to the neutral molecule is stabilized to form the stable base centered radical anion and undergoes bond dissociation process (time scale $> 10^{-13}$ s) as proposed by Simons et al.¹³ and Leszczynski and co-workers.^{16,17} In Table 1, we presented the adiabatic (AEA) and vertical (VEA) electron affinities as computed using B3LYP method and different basis sets. We note for reasons described below the VEAs are not reliable indications of the valence VEAs. The energetics of neutral, anion radical, and transition state (TS) of 5'-dTMPH calculated using B3LYP method and different basis sets (6-31G*, 6-31++G** and DZP++) are given in Table 2.

Electron Affinity of 5'-dTMPH. Using B3LYP/6-31++G** method, the gas-phase AEA of 5'-dTMPH is found to be 0.25 eV, which upon zero-point energy (ZPE) correction becomes 0.40 eV (Table 1). These values are in close agreement as calculated using B3LYP/DZP++ method (0.28 and 0.44 eV (ZPE-corrected))^{16,17} (see Table 1). The calculated VEA by both the methods (B3LYP/6-31++G** and B3LYP/DZP++) were found to be 0.04 and 0.01 eV, respectively. These values are close to zero, and from previous work¹⁹ it is clear that diffuse functions bring in diffuse states (dipole bound and continuum).

Our value is therefore not a reliable value for the valence state VEA. We note that the work of Aflatooni et al.²⁸ reports an experimental (ETS) value of -0.29 eV for the thymine VEA. The predicted AEA of 5'-dTMPH is also found to be very close in value to the AEA (0.31 and 0.44 eV (ZPE-corrected)) of 2'-deoxythymidine (dT) calculated using B3LYP/DZP++ method by Schaefer and co-workers.²⁰ Thus, B3LYP/6-31++G** and B3LYP/DZP++ methods predict that 5'-dTMPH has an energetically stable anion radical when relaxed. The AEA and VEA of 5'-dTMPH calculated using 6-31G* basis set was found to be -0.35 and -1.06 eV, respectively, which is far lower than the expected experimental values. However, as stated above, the corresponding values calculated using 6-31++G** basis set is found to be 0.25 (valence bound) and 0.04 eV with the latter value close in energy to the typical dipole bound state^{22b} and the LUMO shows some diffuse character expected for such a state. The vertical detachment energy (VDE), which is a measure of the electron autodetachment from the anion, is presented in Table 1. The VDE, calculated using B3LYP/6-31++G** and B3LYP/DZP++ methods, of 5'-dTMPH radical anion is found to be 0.97 and 0.99 eV, respectively. These values increase substantially when solvent is included (vide infra).

We note that while smaller basis sets predict less energetically stable anion radicals, these smaller basis sets can be better predictors of relative energetics of valence states than those containing diffuse functions. This problem was treated and discussed in earlier work.¹⁹ Thus, in this work we employed both large and small basis sets to judge the relative energetics in potential energy surfaces and find similar results for valence state portions which adds weight to the predictions made.

Geometries of Neutral, Radical Anion, and Transition State of 5'-dTMPH. The geometries of 5'-dTMPH in their neutral, radical anion, and transition state were fully optimized using B3LYP method and 6-31G* and 6-31++G** basis sets. The B3LYP/6-31++G** optimized structures of neutral, anionic radical, and TS structure of 5'-dTMPH are presented in

TABLE 2: Barrier Heights (kcal/mol) for the C_5-O_5' σ Bond Dissociation of 5'-dTMPH Radical Anion in Their Adiabatic and Vertical States Calculated Using Different Methods

5'-dTMPH	TE (au) ^a			barrier height (kcal/mol)		
	6-31G ^{*b}	6-31++G ^{*b}	DZP++ ^c	6-31G ^{*b}	6-31++G ^{*b}	DZP++ ^c
neutral	-1482.15173	-1482.23842				
anion	-1482.13902	-1482.24765	-1482.45023	0.0	0.0	0.0
TS	-1482.11551	-1482.22621	-1482.42817	14.8 (12.4) ^d	13.5 (11.6) ^d	13.8 (11.9) ^d
anion (vert) ^e	-1482.11266	-1482.23996		9.0 ^f	16.9 ^g	
neutral ^h	-2484.86301					
anion ^h	-2484.90695			28.9		

^a Total energies (atomic unit (au)) calculated using B3LYP method. ^b Present calculation. ^c Ref 16. ^d Zero-point energy (ZPE) corrected value in parenthesis. ^e Anion total energy calculated at the optimized geometry of neutral 5'-dTMPH. ^f Barrier height estimated at 1.7 Å, C_5-O_5' bond stretching (see Figure 3). ^g Barrier height estimated at 1.8 Å, C_5-O_5' bond stretching (see Figure 4). ^h Optimized local minimum structure of neutral and anionic radical of 5'-dTMP in the presence of 11 water molecules and Na^+ as a counterion (Figure 5). Calculation were done using B3LYP/6-31G^{**} method.

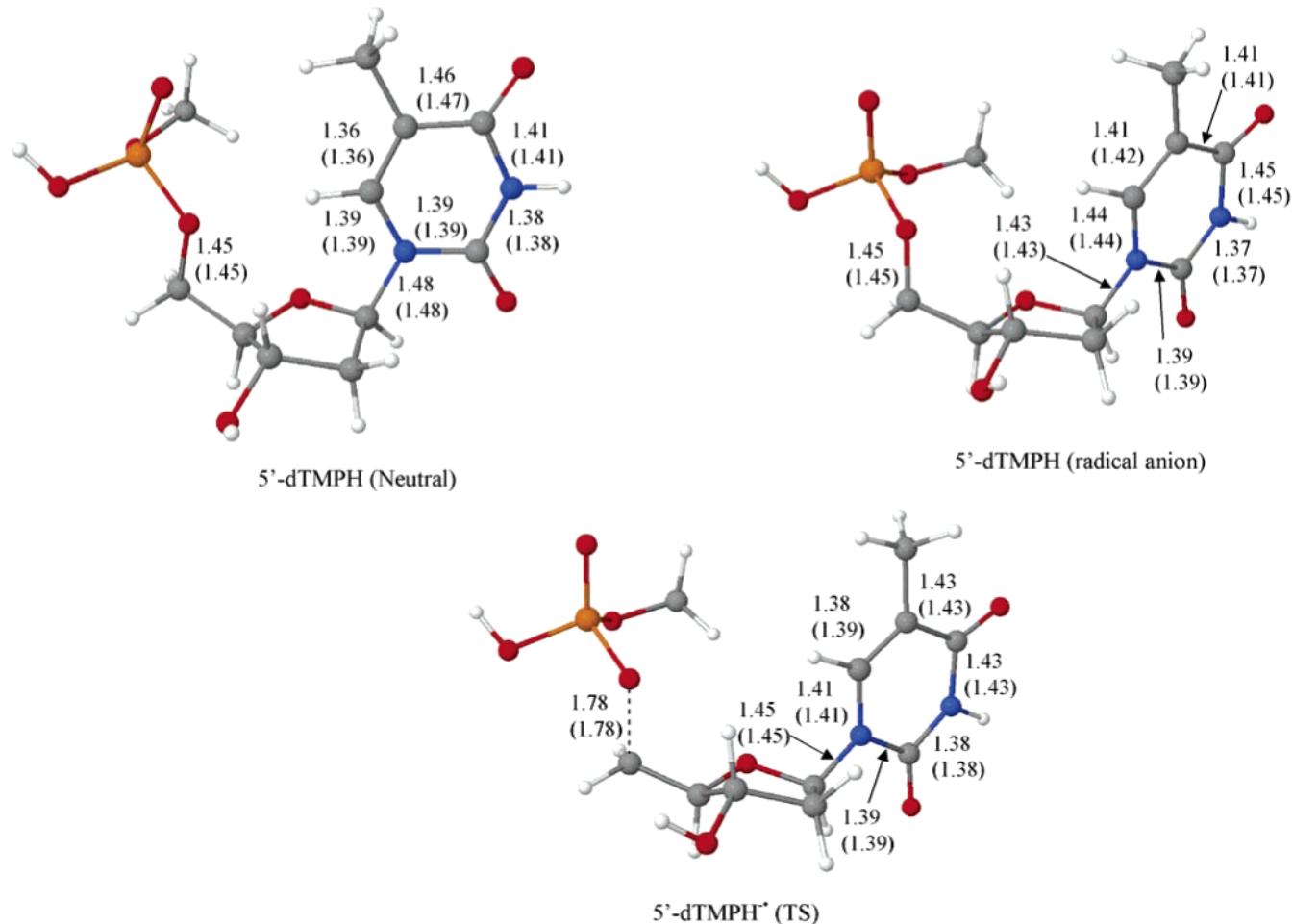


Figure 1. B3LYP/6-31++G^{**} optimized geometries of neutral, anionic radical, and TS of 5'-dTMPH. B3LYP/DZP++ optimized values (ref 16) are given in parentheses. All the distances are given in angstroms (Å).

Figure 1. In Figure 1, we also presented some important geometrical parameters, calculated using B3LYP method and 6-31++G^{**} and DZP++¹⁶ basis sets. As mentioned above we found that both the methods (B3LYP/6-31++G^{**} and B3LYP/DZP++) give the similar values. A maximum bond length difference of ~ 0.05 Å is observed in going from neutral to the radical anion of 5'-dTMPH, which mainly occurs in the thymine part of the 5'-dTMPH (see Figure 1). The transition state for the C_5-O_5' σ bond dissociation is found at 1.78 Å which has an imaginary frequency $782i$ cm^{-1} (Figure 1). Using B3LYP/DZP++ method,¹⁶ the corresponding C_5-O_5' bond distance (in TS) and frequency were found to be 1.78 Å and $758i$ cm^{-1} , respectively. The frequency animation, using JMOL program,³⁴

clearly connects the TS with 5'-dTMPH⁻ (reactant) and the C_5-O_5' bond dissociation which gives products thymidine- C_5' -(HH')-yl and $CH_3OPO_3H^-$, respectively. Using a cytosine-sugar-phosphate DNA fragment, Simons et al.⁹ predicted the corresponding distance ~ 1.9 Å.

Nature of MOs and Virtual Orbital Energies (VOEs) of Neutral 5'-dTMPH. LEEs captured in the lowest unoccupied molecular orbitals (LUMOs) of the neutral molecule results in the formation of transient anions in close to the vertical state. The nature of the wavefunctions associated with the virtual molecular orbitals are of fundamental importance. For this reason, we plotted five LUMOs, including the highest occupied molecular orbital (HOMO) of the neutral 5'-dTMPH, using

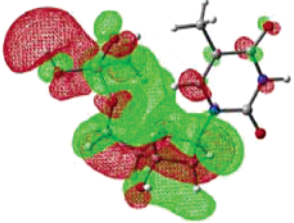
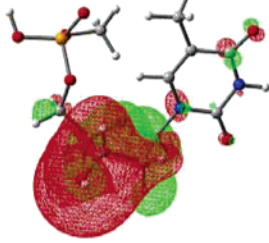
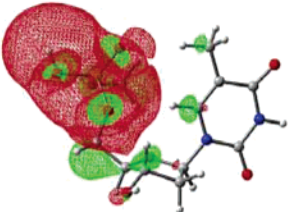
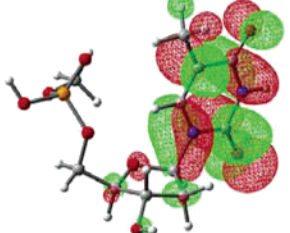
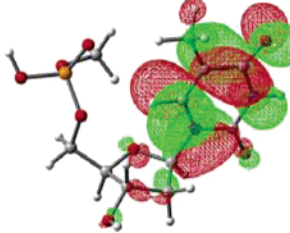
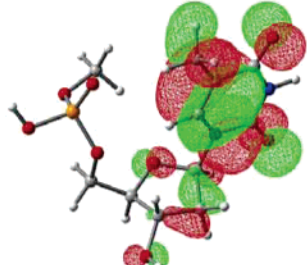
MOs		Orbital Energy (eV)	Scaled VOE (eV)
LUMO + 4 (σ_3^*)		1.78	2.64
LUMO + 3 (σ_2^*)		1.27	2.23
LUMO + 2 (σ_1^*)		0.73	1.80
LUMO + 1 (π_2^*)		0.43	1.56 (1.71)
LUMO (π_1^*)		-0.84	0.53 (0.29)
HOMO (π)		-6.24	

Figure 2. Molecular orbital plots of neutral 5'-dTMPH, calculated using the B3LYP/6-31G* method. B3LYP/6-31G* calculated orbital energies along with scaled values are given in eV. In parentheses, the experimental VOEs of thymine (ref 28) are given in eV.

B3LYP/6-31G* method and shown in Figure 2 with their orbital energies in eV. B3LYP/6-31G* method predicted two lowest π^* orbitals having energies -0.84 and 0.43 eV, respectively. The lowest two σ^* orbitals (Figure 2), having energies 0.73 and 1.27 eV, are localized on the phosphate and sugar group of the 5'-dTMPH (Figure 2), while the lowest third σ^* orbital (1.78 eV) is localized over the whole phosphate and sugar group. It has been observed that within the Koopmans' theorem (KT) approximation, the vertical attachment energies (VAEs) are

equal to the virtual molecular orbitals energies (VOEs) of the neutral molecule. Also, it is found that the VOEs calculated at the Hartree-Fock (HF) level are overestimated than the measured VAEs by several eV.^{30,35,36} However, a linear correlation between the π^* measured VAEs and HF/MP2 computed VOEs has been established with a compact basis sets which do not include diffuse functions.^{30a,35} Recently, the DFT B3LYP/6-31G* method has also been found suitable for the determination of VOEs.^{35c} Using the equation, as used by Modelli,^{35c}

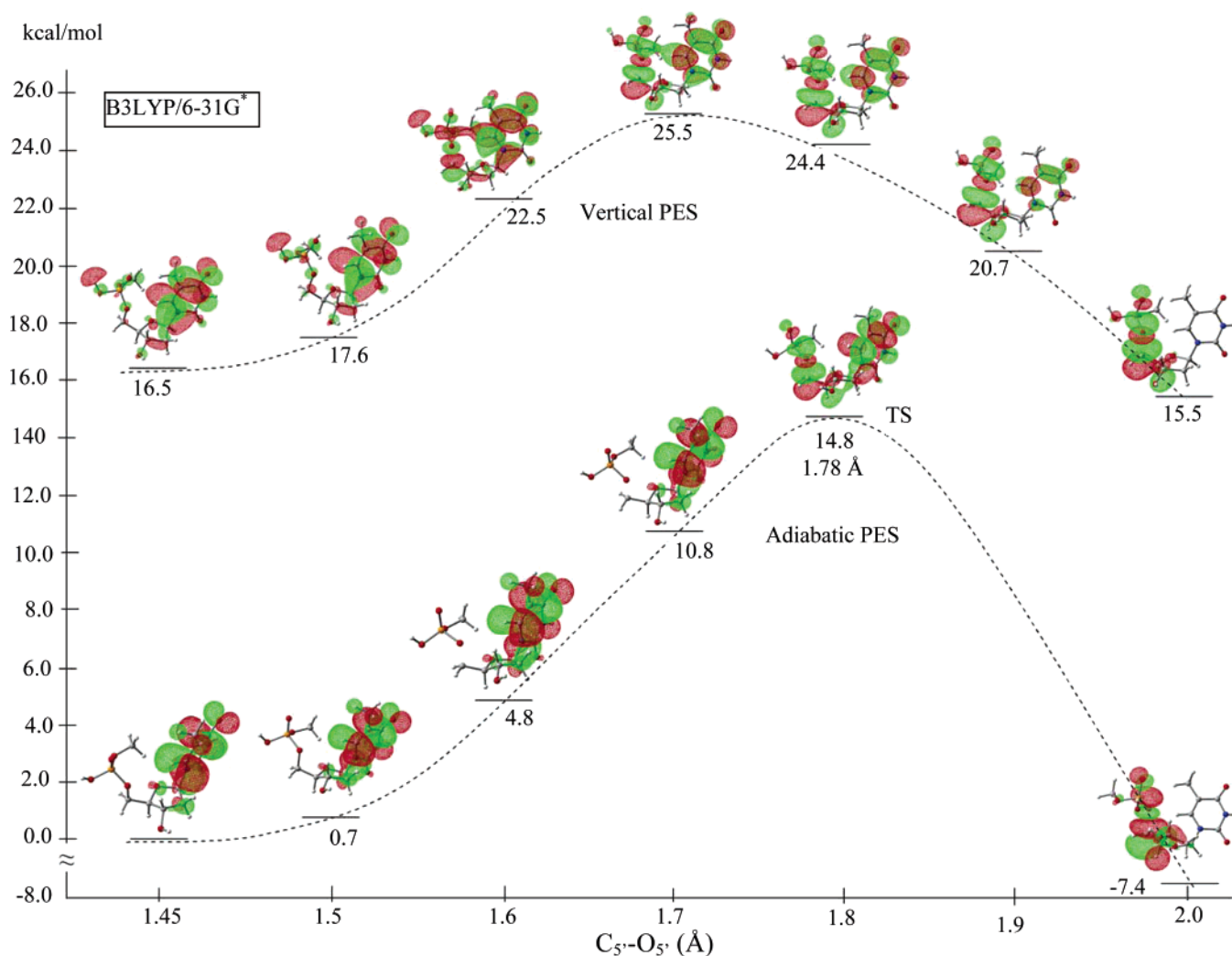


Figure 3. B3LYP/6-31G* calculated adiabatic and vertical potential energy surfaces (PES) of $C_5'-O_5'$ bond dissociation of 5'-dTMPH radical anion. Energies and distances are given in kcal/mol and angstroms (Å), respectively. The singly occupied molecular orbital (SOMO) is also shown.

we obtained the scaled VOs of corresponding B3LYP/6-31G* computed LUMOs of 5'-dTMPH as $0.53(\pi_1^*)$, $1.56(\pi_2^*)$, $1.80(\sigma_1^*)$, $2.23(\sigma_2^*)$, and $2.64(\sigma_3^*)$ eV, respectively. The experimental two lowest π^* orbital VAEs of thymine, using electron transmission spectroscopy (ETS),²⁸ are 0.29 and 1.71 eV, respectively, in reasonable agreement with our calculated π^* VOs. The linear equation^{35c} was derived for π^* VOs, but it works well for σ^* VOs also.²⁷ From scaled VOs, it is noticed that the first lowest σ_1^* orbital VAE 1.80 eV is very close to the second lowest π_2^* orbital VAE which confirms the possibility of the mixing of π^* and σ^* orbitals. In thymine^{30a} the lowest σ^* orbital was found to be localized on the N1-H and C6-H bonds while in 5'-dTMPH the lowest σ^* orbital was localized on the phosphate group (see Figure 2).

$C_5'-O_5'$ Bond Dissociation in Adiabatic and in Vertical States of 5'-dTMPH⁻. To elucidate the mechanism of single strand breaks, we scanned the adiabatic and vertical potential energy surfaces (PESs) by stretching the $C_5'-O_5'$ bond from the equilibrium bond length of neutral and radical anion of 5'-dTMPH to 2.0 Å in 0.1 Å steps (Figures 3 and 4) using both the B3LYP/6-31G* and B3LYP/6-31++G** methods. The vertical and the adiabatic potential energy surfaces (PESs) of $C_5'-O_5'$ bond dissociation are calculated as follows: (i) in the vertical state, single-point energy was calculated at each chosen $C_5'-O_5'$ bond distance on the vertical PES starting with the optimized neutral geometry of 5'-dTMPH and (ii) in the

adiabatic state, the geometry of 5'-dTMPH anionic radical was fully optimized keeping $C_5'-O_5'$ bond distance fixed at each chosen distance on the PES. In Figures 3 and 4, we also present the singly occupied molecular orbitals (SOMOs) in several steps of bond elongation to gain insight into the nature of electron localization during the $C_5'-O_5'$ bond dissociation process.

The adiabatic and vertical PESs, calculated using the B3LYP/6-31G* method, are shown in Figure 3. On the adiabatic PES, the B3LYP/6-31G* calculated TS occurs at a $C_5'-O_5'$ bond distance of 1.78 Å with an activation barrier 14.8 kcal/mol. The calculated TS is characterized by an imaginary frequency $729i$ cm^{-1} . The zero point energy (ZPE) corrected activation barrier is 12.4 kcal/mol (Table 2). Beyond the TS the energy falls rapidly and the process becomes exothermic (Figure 3). Initially the vertical anion starts at a higher energy, i.e., 16.5 kcal/mol above the adiabatic state, Figure 3, as it has not undergone nuclear relaxation. The vertical potential energy surface has a barrier of 9 kcal/mol at 1.7 Å which is ~ 6 kcal/mol lower than the corresponding adiabatic activation barrier. Beyond 1.7 Å the energy falls as in the adiabatic process. The vertical state PES clearly suggests that sufficient excitation of the $C_5'-O_5'$ bond can result in bond cleavage without nuclear relaxation with a quite low barrier height which suggests a facile and rapid process in the transient anion is possible.

In Figure 4, we presented the B3LYP/6-31++G** calculated PES of adiabatic and vertical dissociation of $C_5'-O_5'$ σ bond

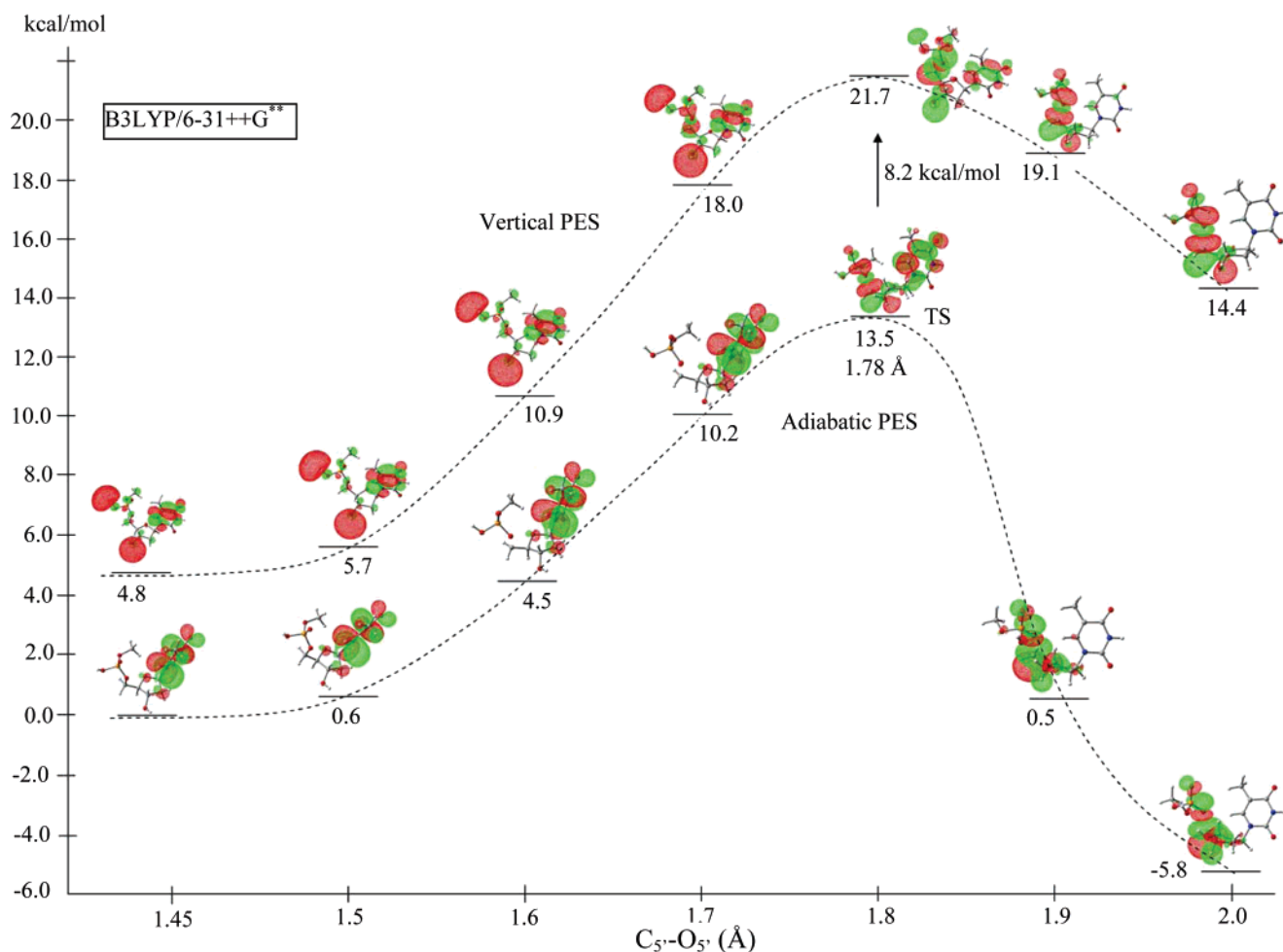


Figure 4. B3LYP/6-31++G** calculated adiabatic and vertical potential energy surfaces (PES) of $C_{5'}-O_{5'}$ bond dissociation of 5'-dTMPH radical anion. Energies and distances are given in kcal/mol and angstroms (Å), respectively. The singly occupied molecular orbital (SOMO) is also shown.

of 5'-dTMPH $^{\cdot-}$. For the adiabatic PES, we find the calculated transition state (TS) has an activation energy of 13.5 kcal/mol and characterized with an imaginary frequency of $782i\text{ cm}^{-1}$ and $C_{5'}-O_{5'}$ bond distance 1.78 Å. Inclusion of the ZPE correction lowers activation barrier to 11.6 kcal/mol (Table 2). Previous efforts using the B3LYP/DZP++ method¹⁶ found similar values of activation energy and $C_{5'}-O_{5'}$ bond distance in the TS (Table 2, and Figures 1, 4). The B3LYP/6-31++G** calculated vertical state of the 5'-dTMPH radical anion lies only 4.8 kcal/mol above the adiabatically relaxed radical anion, shown in Figure 4. A comparative analysis of the vertical PES with adiabatic PES (Figure 4) clearly demonstrates that the PES in both the states has similar shape and nature from energetic points of view. In the vertical state, we found that activation barrier occurred at ~ 17.0 kcal/mol, which is 3.5 kcal/mol higher than the adiabatic TS barrier height of 5'-dTMPH radical anion (see Figure 4 and Table 2) at the same level of calculation. The $C_{5'}-O_{5'}$ bond distance corresponding to the vertical activation barrier lies at ~ 1.8 Å, which is about the adiabatic TS value of 1.78 Å.

A comparison of the results for the two basis sets shows that they are similar in shape and energetics (Figures 3 and 4). Although the 6-31++G** basis set gives nearly the same barrier for the adiabatic pathway as the 6-31G*, a higher barrier for the vertical pathway is found for the 6-31++G** basis set. Usually the larger basis set gives the best energetics for a PES; however, for systems which have EA near zero, this may not be the case. For the larger 6-31++G** basis set, the diffuse

functions mix in dipole bound and continuum states for the vertical PES which artificially lowers the starting position for the vertical anion radical and do not reflect the virtual π^* state energy. Thus, we believe the vertical anion PES shape and barrier is likely best described by the smaller basis set. We note that at the TS and after (where the electron is captured in the σ^* dissociative valence state) differences in energy between vertical and adiabatic surfaces for both basis sets are in excellent agreement. For example, at the TS the difference between vertical and adiabatic PESs is 8.2 kcal/mol for the 6-31++G** basis set and about 10 kcal/mol for the 6-31G* basis set and at 2 Å the differences are 20.2 kcal/mol and 22.9 kcal/mol, respectively.

Solvation Effects on the PES Surface for $C_{5'}-O_{5'}$ Bond Dissociation in 5'-dTMPH $^{\cdot-}$. It is well-known that electron affinities increase with solvation mainly by the solvent polarization (Born term). This results in a substantial increase (by several eV) over corresponding gas-phase EA values.^{21,37-40} For example, using the static IPCM model for water ($\epsilon = 78.39$), Gu et al.³⁸ reported that the stability of the anion radical of 5'-dTMPH increased to 2.0 eV AEA and 1.44 eV VEA. While the IPCM model is adequate for bulk solvent effects, for hydrogen bonding solvents such as water, it neglects the specific local interactions and hydrogen-bonding energetics, which are substantial contributions to solvation energetics and are critical in determining reaction pathways. This level of sophistication is usually avoided owing to the complexity increase in the treatment. In order to gain some understanding of the PES in

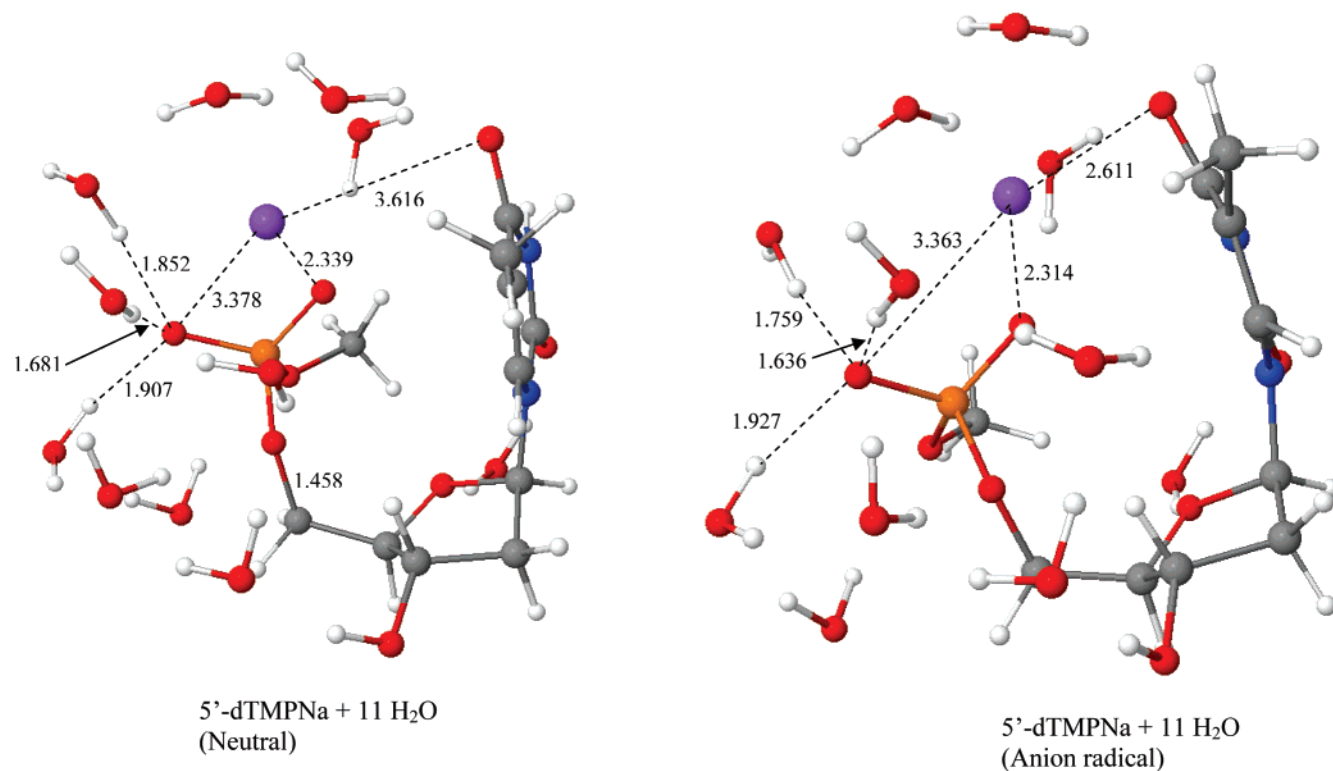


Figure 5. B3LYP/6-31G** optimized geometries of neutral and anionic radical of 5'-dTMP with Na⁺ as a counterion in the presence of 11 water molecules.

an aqueous environment, in this work we have chosen to consider a model that includes a solvation shell of waters and a sodium counterion. We note that for a full understanding of the effect of solvent, molecular dynamics simulation methods are more appropriate to describe the numerous conformations that exist albeit a narrow energy range while the conventional ab initio or DFT methods provide only a single local minimum configuration. But our work, presented below, shows the overall barrier to dissociation increases with hydration significantly even with only five waters of hydration.

Two hydrated structures were considered 5'-dTMP with 5 water molecules and Na⁺ and 5'-dTMP with 11 water molecules and a Na⁺. Surprisingly, both give similar results. We first consider the larger 11 water system. The initial structure of the 5'-dTMP with 11 water molecules and a Na⁺ was generated using GaussView³³ as follows: we placed Na atom 2.2 Å away from each of the two oxygen atoms of the PO₄ group of the 5'-dTMP. Also, the Na atom lies almost in the plane of the O–P–O atoms and the maximum deviation from planarity was ~6°, respectively. Near both the oxygen atoms of the thymine moiety single water molecule was placed in the hydrogen-bonding configuration as observed experimentally by X-ray crystallography.^{41a} One water molecule was placed in the hydrogen-bonding configuration near the O_{3'}-H bond of the sugar.^{41a} Since sugar and PO₄ group are exposed to the solvent,^{41b} we placed eight water molecules around the PO₄ group. Recent X-ray crystallographic analysis of the hydration of A- and B-DNA at atomic level has been studied by Egli et al.^{41a} In their^{41a} study they found that largest number of waters in the first hydration shell were found near the PO₄ group. Schneider et al.^{41c} showed that a minimum of six water molecules are required to solvate the charged oxygens of the PO₄ group. An early theoretical study^{41d} predicted that six water molecules would constitute the first hydration shell of a PO₄ group has been confirmed by experiment,^{41e} molecular dynamics simulation^{41c,f} and solution NMR.^{41g} To ensure the intercon-

vertability between the anion and the neutral systems, the optimized neutral system was obtained by considering the corresponding optimized radical anion structure as the initial structure for the neutral state. We also optimized the geometries of 5'-dTMP considering Na⁺ as a counterion in gas-phase (without water molecules) in the neutral and anionic states using the B3LYP/6-31++G** method. However, for this case, addition of an electron produced a neutral Na instead of the base anion radical, and this was not considered further (see supplement Figures S1 and S2). The optimized geometries of neutral and anion radical with 11 water molecules are presented in Figure 5. In the neutral state of 5'-dTMPNa + 11H₂O, the Na atom lies near the oxygen atoms of the PO₄ group and the Na–O bond distances are 2.339 and 3.378 Å, respectively, and the corresponding Na–O bond distances in the anionic state were found to be 2.314 and 3.363 Å, respectively. From the optimized structures of 5'-dTMPNa + 11H₂O in neutral and anion radical, we also found that three water molecules are hydrogen bonded with distances in the range 1.64–1.9 Å to one of the oxygen atoms of the PO₄ group. This forms a cone of hydration (see Figure 5) as observed experimentally,^{41c,e} in molecular dynamics simulation study^{41c,f} and studied recently using the B3LYP/6-31G(d) method.^{41h} It is found by X-ray crystallography^{41a} that the distance between Na⁺ and oxygen atom is around 2.4 Å which is nicely predicted by the theory. In anionic state of 5'-dTMPNa + 11H₂O, we see from Figure 5 that though Na atom lies near the oxygen atom of PO₄ but it shifts toward the thymine moiety. It is apparent that in anionic state of 5'-dTMPNa + 11H₂O, the Na⁺ is attracted both by the negatively charged oxygens of PO₄ group and the anionic thymine base.

Our results show that solvent has a pronounced effect on the stability of the radical anion in comparison to the corresponding neutral molecule and the calculated AEA of 5'-dTMP was found to be 1.20 eV. Further, to consider the effect of the full solvent on the stability of the 5'-dTMPNa + 11 H₂O, we performed

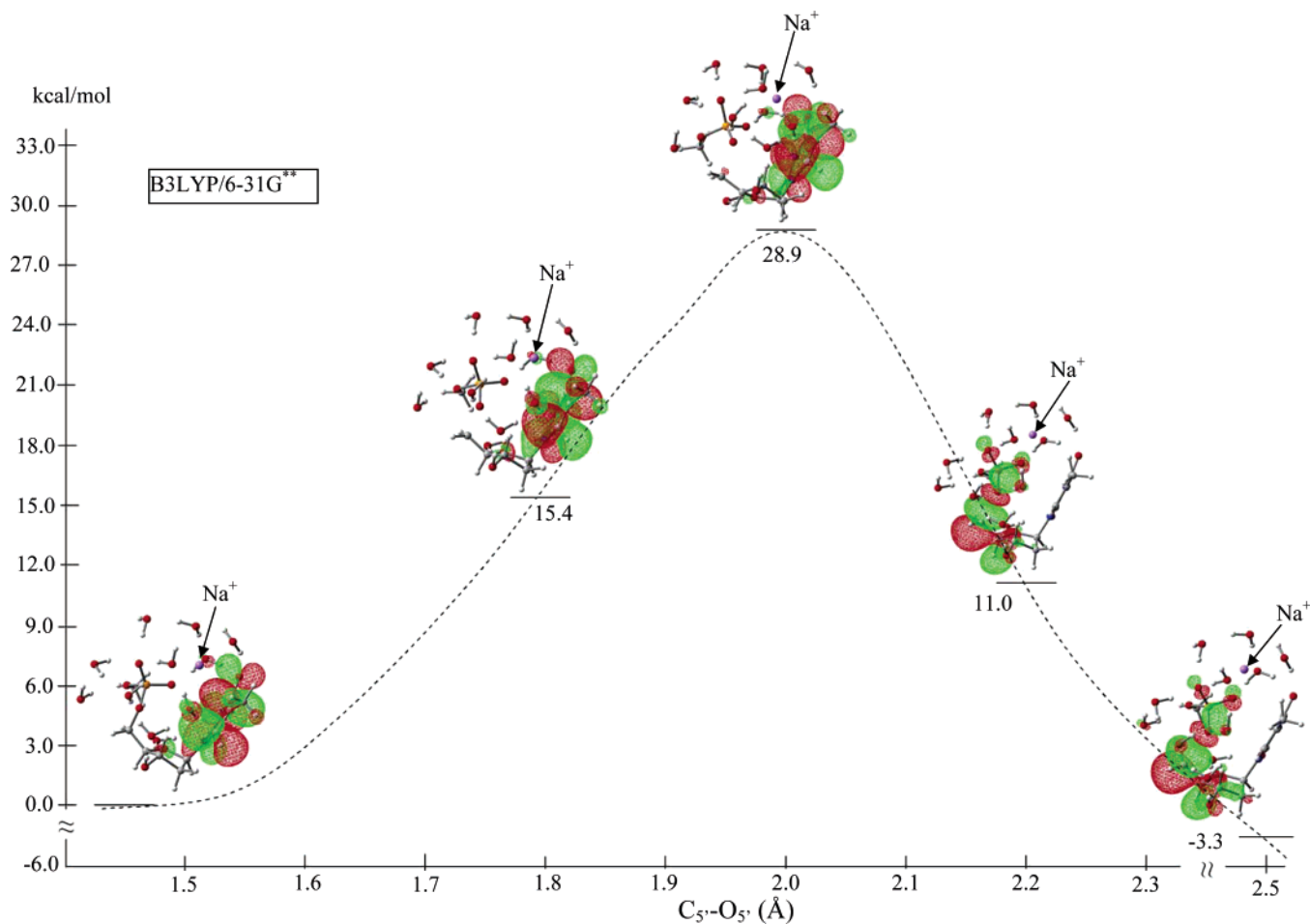


Figure 6. B3LYP/6-31G** calculated adiabatic potential energy surface (PES) of $C_5'-O_5'$ bond dissociation of 5'-dTMP radical anion in the presence of 11 water molecules and Na^+ as a counterion. Energies and distances are given in kcal/mol and angstroms (\AA), respectively. The singly occupied molecular orbital (SOMO) is also shown.

single-point calculation using polarized continuum model (PCM) as solvent with $\epsilon = 78.39$. We found that the AEA of 5'-dTMPNa radical anion in the bulk solvent increases appreciably and attains the value of 2.17 eV (see Table 1). This value is in close agreement with those reported by Gu et al.³⁸ We also computed the adiabatic PES of $C_5'-O_5'$ bond dissociation and estimated the barrier of ~ 30.0 kcal/mol at a distance of 2.0 \AA (see Figure 6) using B3LYP/6-31G** level of theory. The computed barrier height and the dissociation distance (~ 2 \AA) are appreciably larger than the corresponding gas-phase values (Table 2 and Figures 3, 4). In each step of $C_5'-O_5'$ bond dissociation, we also plotted the SOMO to see the nature of excess electron localization during bond rupture process. In the optimized local minimum conformation of solvated 5'-dTMPNa radical anion, we see the SOMO is localized on the thymine shown in Figure 6 and is still localized on the thymine up to and including the top of the barrier at 2 \AA (Figure 6). However, we note that for the gas-phase calculation for 5'-dTMPH the electron is fully transferred into the $C_5'-O_5'$ bond at the TS (see Figures 3, 4). For the solvated system, the transfer of the excess electron from thymine to the $C_5'-O_5'$ bond region only takes place beyond 2 \AA and water molecules then shift toward the PO_4 moiety to solvate it. It is likely the substantial solvent reorganization associated with the electron transfer from thymine to the $C_5'-O_5'$ bond provides the majority of the large increase in activation barrier.

To check that a similar effect, as described above for 5'-dTMPNa + 11 H_2O radical anion, can be reproduced with fewer

water molecules around the PO_4 group, we optimized the structures of 5'-dTMPNa in the presence of only five water molecules in the neutral and in the anionic radical states using the B3LYP/6-31G** level of theory. In this case, four water molecules were placed near the phosphate group while one water molecule was placed near the oxygen atom of the thymine base. In this case also we found the similar result as predicted with the larger solvated system (11 water molecules, Figure 6). In the adiabatic state, the barrier for $C_5'-O_5'$ bond dissociation of 5'-dTMPNa + 5 H_2O radical anion occurs at 1.9 \AA having barrier height 26.0 kcal/mol. Also, the excess electron transfers from the thymine base to the $C_5'-O_5'$ bond region beyond 1.9 \AA . The PES of $C_5'-O_5'$ bond dissociation of 5'-dTMPNa + 5 H_2O radical anion along with the SOMOs are presented in Figures S5 and S6 in the Supporting Information.

The calculated VDEs of 5'-dTMPNa + 5 H_2O and 5'-dTMPNa + 11 H_2O radical anions were found to be 2.19 and 2.60 eV, respectively. The corresponding VDEs in the presence of bulk solvent (PCM model) are found to be 3.05 and 3.20 eV, respectively, (see Table 1). In comparison to the gas-phase, the vertical detachment energies (VDEs) of the 5'-dTMP radical anion in the solvated environment enhanced appreciably, which shows that the excess electron in the solvated anion radical is highly stable toward detachment.

Conclusions

From the previous works of Burrow et al.^{28,36} and Sanche et al.⁴² it is clear that LEE attachment can excite specific

vibrational modes even in the condensed state.⁴² Thus it is expected that LEEs may excite vibrational modes which lead directly the bond elongation and bond cleavage which for some pathways would have low barriers as found in this work. An earlier proposed mechanism^{9–14,16,17} of SSB, proceeding fully on the adiabatic surface, is unlikely to occur in an aqueous environment.^{9–14,16,17} We find the adiabatic barrier in a model aqueous environment is quite high (ca. 30 kcal/mol) results from the adiabatic solvation of the thymine base anion radical which provides a significant barrier to the electron transfer to the extended C_{5'}–O_{5'} in the sugar phosphate backbone. This pathway will therefore not significantly contribute to bond cleavage. This is in accord with the work of Simons et al.¹¹ who calculated that at the barrier height of 25 kcal/mol the C_{5'}–O_{5'} σ bond cleavage rate was 10⁻⁵ s⁻¹ even for a 1 eV electron.¹¹ It is also in accord with experiments that show DNA strand breakage by solvated electrons is not observed in aqueous solution.^{1c, 1d}

We note that on a time scale appropriate for transition states (<10⁻¹² s), specific vibrational motions will dominate.⁴³ A mechanism in which transient anion formation the C_{5'}–O_{5'} bond is vibrationally excited and induces the bond dissociation process appears quite probable. In this model, it is difficult to account for how the C_{5'}–O_{5'} bond is vibrationally excited while the electron forms the transient ion mainly on the DNA base. The direct attachment to the phosphate might then seem more likely to have such an effect and our results shown in Figure 2 indicate below 2 eV there are states available on the phosphate. Using theoretical modeling of resonant electron scattering from DNA, Caron and Sanche⁴⁴ found the probability of electron localization at the phosphate group was so high that they concluded “any transient anion state formed by electron capture at the phosphate group with a longer lifetime or of the order of the C–O bond vibrations within DNA is expected to contribute significantly to SSB”.⁴⁴ While recent observations by Sanche et al.,^{44–46} Märk, Illenberger and co-workers^{7,24} suggest that the sugar phosphate may be a site for LEE attack there are experiments that suggest the point of attachment is at the DNA bases as well.^{4e} Our work provides some insight into the energetics available in the vertical and adiabatic pathways after electron addition to the base and future work will be needed to further elucidate this highly interesting problem.

Acknowledgment. This work was supported by the NIH NCI under Grant No. R01CA045424. The authors are grateful to the Artic Region Supercomputing Center (ARSC) for generously providing the computational time to perform these calculations. The authors also thank the ARSC staff for their support and cooperation. We thank the reviewers of this work, whose comments led us to perform the calculation of five water molecules associated with 5'-dTMPNa.

Supporting Information Available: Full ref 32 and figures showing optimized geometries, SOMOs, and PESs. This material is available free of charge via the Internet at <http://pubs.acs.org>.

References and Notes

(1) (a) In *Radiation Damage in DNA: Structure/Function Relationships at Early Times*; Fuciarelli, A. F., Zimbrick, J. D., Eds.; Battelle: Columbus, OH, 1995. (b) von Sonntag, C. *The Chemical Basis for Radiation Biology*; Taylor and Francis: London, 1987. (c) von Sonntag, C. *Free-Radical-Induced DNA Damage and Its Repair*; Springer-Verlag: Berlin, 2006; p 82 (d) Myers, L. S., Jr.; Kay, E. *Int. J. Radiat. Oncol. Biol. Phys.* **1979**, *5*, 1055.

(2) (a) Becker, D.; Sevilla, M. D. *Electron Spin Reson.* **1998**, *16*, 79. (b) Sevilla, M. D.; Becker, D. *Electron Spin Reson.* **2004**, *19*, 243. (c) Cai, Z.; Sevilla, M. D. *Top. Curr. Chem.* **2004**, *237*, p 103. (d) von Sonntag, C. *Free-Radical-Induced DNA Damage and Its Repair*; Springer-Verlag: Berlin, 2006; p 213.

(3) (a) Sevilla, M. D.; Becker, D.; Yan, M.; Summerfield, S. R. *J. Phys. Chem.* **1991**, *95*, 3409. (b) Yan, M.; Becker, D.; Summerfield, S. R.; Renke, P.; Sevilla, M. D. *J. Phys. Chem.* **1992**, *96*, 1983. (c) Wang, W.; Sevilla, M. D. *Radiat. Res.* **1994**, *9*, 17. (d) Spaletta, R. A.; Bernhard, W. A. *Radiat. Res.* **1993**, *143*.

(4) (a) Boudaïffa, B.; Cloutier, P.; Hunting, D.; Huels, M. A.; Sanche, L. *Science* **2000**, *287*, 1658. (b) Huels, M. A.; Boudaïffa, B.; Cloutier, P.; Hunting, D.; Sanche, L. *J. Am. Chem. Soc.* **2003**, *125*, 4467. (c) Zheng, Y.; Cloutier, P.; Hunting, D. J.; Wagner, J. R.; Sanche, L. *J. Am. Chem. Soc.* **2004**, *126*, 1002. (d) Martin, F.; Burrow, P. D.; Cai, Z.; Cloutier, P.; Hunting, D.; Sanche, L. *Phys. Rev. Lett.* **2004**, *93*, 068101 (e) Zheng, Y.; Cloutier, P.; Hunting, D. J.; Sanche, L.; Wagner, J. R. *J. Am. Chem. Soc.* **2005**, *127*, 16592.

(5) (a) LaVerne, J. A.; Pimblott, S. M. *Radiat. Res.* **1995**, *141*, 208. (b) Hotop, H.; Ruf, M.-W.; Allan, M.; Fabrikant, I. I. *Adv. At. Mol. Opt. Phys.* **2003**, *49*, 85.

(6) (a) Hanel, G.; Denifl, S.; Scheier, P.; Probst, M.; Farizon, B.; Farizon, M.; Illenberger, E.; Märk, T. D. *Phys. Rev. Lett.* **2003**, *90*, 188104. (b) Denifl, S.; Ptasińska, S.; Cingel, M.; Matejčík, S.; Scheier, P.; Märk, T. D. *Chem. Phys. Lett.* **2003**, *377*, 74. (c) Abouaf, R.; Pommier, J.; Dunet, H. *Int. J. Mass Spectrom.* **2003**, *226*, 397. (d) Abdoul-Carime, H.; Gohlke, S.; Illenberger, E. *Phys. Rev. Lett.* **2004**, *92*, 168103. (e) Denifl, S.; Ptasińska, S.; Probst, M.; Hrusak, J.; Scheier, P.; Märk, T. D. *J. Phys. Chem. A* **2004**, *108*, 6562. (f) Ptasińska, S.; Denifl, S.; Mróz, B.; Probst, M.; Grill, V.; Illenberger, E.; Scheier, P.; Märk, T. D. *J. Chem. Phys.* **2005**, *123*, 124302. (g) Ptasińska, S.; Denifl, S.; Scheier, P.; Illenberger, E.; Märk, T. D. *Angew. Chem.* **2005**, *117*, 7101; *Angew. Chem., Int. Ed.* **2005**, *44*, 6941.

(7) Bald, I.; Kopyra, J.; Illenberger, E. *Angew. Chem., Int. Ed.* **2006**, *45*, 4851.

(8) (a) Li, X.; Sanche, L.; Sevilla, M. D. *Radiat. Res.* **2006**, *165*, 721. (b) Li, X.; Sevilla, M. D. *Adv. Quantum Chem.* **2007**, *52*, 59. (c) Li, X.; Sevilla, M. D.; Sanche, L. *J. Phys. Chem. B* **2004**, *108*, 19013. (d) Li, X.; Sevilla, M. D.; Sanche, L. *J. Am. Chem. Soc.* **2003**, *125*, 13668.

(9) Simons, J. *Acc. Chem. Res.* **2006**, *39*, 772.

(10) Berdys, J.; Anusiewicz, I.; Skurski, P.; Simons, J. *J. Am. Chem. Soc.* **2004**, *126*, 6441.

(11) Anusiewicz, I.; Berdys, J.; Sobczyk, M.; Skurski, P.; Simons, J. *J. Phys. Chem. A* **2004**, *108*, 11381.

(12) Berdys, J.; Anusiewicz, I.; Skurski, P.; Simons, J. *J. Phys. Chem. A* **2004**, *108*, 2999.

(13) Barrios, R.; Skurski, P.; Simons, J. *J. Phys. Chem. B* **2002**, *106*, 7991.

(14) Berdys, J.; Skurski, P.; Simons, J. *J. Phys. Chem. B* **2004**, *108*, 5800.

(15) Gu, J.; Xie, Y.; Schaefer, H. F. *J. Am. Chem. Soc.* **2005**, *127*, 1053.

(16) Bao, X.; Wang, J.; Gu, J.; Leszczynski, J. *Proc. Nat. Acad. Sci. U.S.A.* **2006**, *103*, 5658.

(17) Gu, J.; Wang, J.; Leszczynski, J. *J. Am. Chem. Soc.* **2006**, *128*, 9322.

(18) Wesolowski, S. S.; Leininger, M. L.; Pentchev, P. N.; Schaefer, H. F. *J. Am. Chem. Soc.* **2001**, *123*, 4023.

(19) Li, X.; Cai, Z.; Sevilla, M. D. *J. Phys. Chem. A* **2002**, *106*, 1596.

(20) Richardson, N. A.; Gu, J.; Wang, S.; Xie, Y.; Schaefer, H. F. *J. Am. Chem. Soc.* **2004**, *126*, 4404.

(21) Gu, J.; Xie, Y.; Schaefer, H. F. *J. Am. Chem. Soc.* **2006**, *128*, 1250.

(22) (a) Schiedt, J.; Weinkauff, R.; Neumark, D.; Schlag, E. *Chem. Phys.* **1998**, *239*, 511 (b) Hendricks, J. H.; Lyapustina, S. A.; de Clercq, H. L.; Snodgrass, J. T.; Bowen, K. H. *J. Chem. Phys.* **1996**, *104*, 7788.

(23) Hanel, G.; Gstir, B.; Denifl, S.; Scheier, P.; Probst, M.; Farizon, B.; Farizon, M.; Illenberger, E.; Märk, T. D. *Phys. Rev. Lett.* **2003**, *90*, 188104.

(24) Ptasińska, S.; Denifl, S.; Gohlke, S.; Scheier, P.; Illenberger, E.; Märk, T. D. *Angew. Chem., Int. Ed.* **2006**, *45*, 1893.

(25) König, C.; Kopyra, J.; Bald, I.; Illenberger, E. *Phys. Rev. Lett.* **2006**, *97*, 018105.

(26) Schulz, G. *J. Rev. Mod. Phys.* **1973**, *45*, 423.

(27) (a) Modelli, A.; Jones, D. *J. Phys. Chem. A* **2006**, *110*, 10219. (b) Modelli, A.; Jones, D. *J. Phys. Chem. A* **2006**, *110*, 13195.

(28) Aflatoon, K.; Gallup, G. A.; Burrow, P. D. *J. Phys. Chem. A* **1998**, *102*, 6205.

(29) Sevilla, M. D.; Besler, B.; Colson, A.-O. *J. Phys. Chem.* **1995**, *99*, 1060.

(30) (a) Burrow, P. D.; Gallup, G. A.; Scheer, A. M.; Denifl, S.; Ptasińska, S.; Märk, T.; Scheier, P. *J. Chem. Phys.* **2006**, *124*, 124310. (b) Scheer, A. M.; Silvernail, C.; Belot, J. A.; Aflatoon, K.; Gallup, G. A.; Burrow, P. D. *Chem. Phys. Lett.* **2005**, *411*, 46. (c) Scheer, A. M.; Aflatoon,

- K.; Gallup, G. A.; Burrow, P. D. *Phys. Rev. Lett.* **2004**, *92*, 068102. (d) Aflatooni, K.; Scheer, A. M.; Burrow, P. D. *J. Chem. Phys.* **2006**, *125*, 054301.
- (31) Rienstra-Kiracofe, J. C.; Tschumper, G. S.; Schaefer, H. F.; Nandi, S.; Ellison, G. B. *Chem. Rev.* **2002**, *102*, 231.
- (32) Frisch, M. J.; et al. *Gaussian03*, Revision B.04; Gaussian, Inc.: Pittsburgh, PA, 2003.
- (33) *GaussView*; Gaussian, Inc.: Pittsburgh, PA, 2003.
- (34) <http://jmol.sourceforge.net>. Jmol development team, An Open-Science Project © 2004.
- (35) (a) Chen, D.; Gallup, G. A. *J. Chem. Phys.* **1990**, *93*, 8893. (b) Staley, S. W.; Strand, J. T. *J. Phys. Chem.* **1994**, *98*, 116. (c) Modelli, A. *Phys. Chem. Chem. Phys.* **2003**, *5*, 2923.
- (36) (a) Jordan, K. D.; Burrow, P. D. *Acc. Chem. Res.* **1978**, *11*, 341. (b) Jordan, K. D.; Burrow, P. D. *Chem. Rev.* **1987**, *87*, 557.
- (37) Mazurkiewicz, K.; Maciej, Harańczyk, M.; Gutowski, M.; Rak, J.; Radisic, D.; Eustis, S. N.; Wang, D.; Bowen, K. H. *J. Am. Chem. Soc.* **2007**, *129*, 1216.
- (38) Gu, J.; Xie, Y.; Schaefer, H. F. *Chem. Phys. Chem.* **2006**, *7*, 1885.
- (39) Kumar, A.; Mishra, P. C.; Suhai, S. *J. Phys. Chem. A* **2005**, *109*, 3971.
- (40) Kim, S.; Wheeler, S. E.; Schaefer, H. F. *J. Chem. Phys.* **2006**, *124*, 204310.
- (41) (a) Egli, M.; Tereshko, V.; Teplova, M.; Minasov, G.; Joachimiak, A.; Sanishvili, R.; Weeks, C. M.; Miller, R.; Maier, M. A.; An, H. Y.; Cook, P. D.; Manoharan, M. *Biopolymers* **1998**, *48*, 234. (b) Liu, D.; Wyttenbach, T.; Bowers, M. T. *J. Am. Chem. Soc.* **2006**, *128*, 15155. (c) Schneider, B.; Patel, K.; Berman, H. M. *Biophys. J.* **1998**, *75*, 2422. (d) Pullman, B.; Pullman, A.; Berthod, H.; Gresh, N. *Theor. Chim. Acta* **1975**, *40*, 93. (e) Westhof, E. Structural water bridges in nucleic acids. In *Water and Biological Macromolecules*; Westhof, E., Ed.; CRC Press: Boca Raton, FL, 1993; Vol. 5, pp 226–243. (f) Duan, Y.; Wilkosz, P.; Crowley, M.; Rosenberg, J. M. *J. Mol. Biol.* **1997**, *272*, 553. (g) Kochoyan, M.; Leroy, J. L. *Curr. Opin. Struct. Biol.* **1995**, *5*, 329. (h) Přecechtělová, J.; Munzarová, M. L.; Novák, P.; Sklenář, V. *J. Phys. Chem. B* **2007**, *111*, 2658.
- (42) Levesque, P. L.; Michaud, M.; Sanche, L. *Nucl. Instrum. Methods Phys. Res. B* **2003**, *208*, 225.
- (43) Zewail, A. H. *J. Phys. Chem. A* **2000**, *104*, 5660.
- (44) Caron, L.; Sanche, L. *Phys. Rev. A* **2005**, *72*, 032726.
- (45) Možeško, P.; Sanche, L. *Radiat. Phys. Chem.* **2005**, *73*, 77.
- (46) Pan, X.; Sanche, L. *Chem. Phys. Letts.* **2006**, *421*, 404.